*Earth Planets Space*, **60**, 949–960, 2008

# Interaction of Alfven waves with a turbulent layer

V. Pilipenko[1], E. Fedorov[2], and M. J. Engebretson[3]

[1]*Space Research Institute, 84/32 Profsojuznaya, Moscow 117997, Russia*
[2]*Institute of the Physics of the Earth, 10 B. Gruzinskaya, Moscow 123995, Russia*
[3]*Augsburg College, 2211 Riverside Ave., Minneapolis, MN 55454*

(Received March 6, 2008; Revised June 6, 2008; Accepted June 23, 2008; Online published October 15, 2008)

We consider the interaction of Alfven waves with a resistive turbulent layer with anomalous conductivity. High-frequency turbulence causes the occurrence of both field-aligned and transverse resistivity. The correct dispersion relationship for Alfven waves in a turbulent medium with anisotropic conductivities has been derived. Alfven waves may partially reflect from a resistive layer, be absorbed in it, or be transmitted through it. When field-aligned resistivity dominates, the relative effectiveness of these processes critically depends on the wave transverse scale. For a thin layer as compared with the wave field-aligned length, the characteristic parameter that controls the effectiveness of the wave interaction with a layer is the resistive Alfven scale $\lambda_A$, determined by the field-aligned resistance and Alfven velocity above the layer. Comparison of energy losses estimated from analytical relationships for a "thin" layer and from numerical calculations for a finite width layer shows that the thin layer approximation provides a reasonable estimate over a wide range of wave scales, not only very small. Estimation of the effective damping scale of the Pc1 waves in a turbulent cusp shows that the cusp proper cannot be a conduit of Pc1 wave energy from the magnetosheath to the ground. The "thin" layer model has been applied to the interpretation of the results of early studies of transient ULF wave (Pi2 pulsations) damping during substorm onset, which showed that the damping rate increased for accompanying magnetic bays stronger than $\sim$100 nT. Our estimates confirm that this additional damping can be caused by the occurrence of anomalous transverse resistance when magnetospheric current exceeds the threshold necessary for the excitation of high-frequency plasma turbulence.

**Key words:** Alfven waves, ULF pulsations, anomalous resistivity, plasma turbulence.

## 1. Introduction

Alfven waves play an important role in dynamic processes in space plasma by transporting without geometric attenuation non-stationary field-aligned currents to considerable distances. Space plasma is often turbulent, so scattering of particles by turbulent noise becomes more efficient than Coulomb collisions. Such anomalous collisions of particles with turbulent noise result in the occurrence of finite anomalous plasma resistivity (Galeev and Sagdeev, 1973; Liperovsky and Pudovkin, 1983) and formation of turbulent layers (TL) in a space plasma.

The problem considered here is just one aspect of the more fundamental problem of MHD wave propagation through a turbulent plasma. This latter, still not resolved problem is of key importance for near-Earth space physics, in particular for penetration of ULF waves through the magnetosheath or auroral plasma, propagation of ULF bursts and transients along the magnetotail, etc.

For the problem of energy transfer in space the interaction of Alfven waves with a region of turbulent plasma with finite conductivity due to anomalous collisions is of great importance. The basic notions about Alfven wave interaction with a turbulent layer (TL) with anomalous field-aligned resistance were formulated by Lysak and Dum (1983), who showed that waves can partially penetrate a layer, be absorbed in it, and reflect from it. The relative rate of these processes turned out to be dependent on the transverse wave scale. Later on this model was augmented by Trakhtenhertz and Feldstein (1985), who indicated that the occurrence of anomalous collisions should modify not only the field-aligned conductivity, but transverse (Pedersen) conductivity as well, and substantially enhance the wave absorption in a TL.

Quite often, e.g. at auroral latitudes, the high-frequency turbulence is confined in a narrow region, where the threshold for current instability is minimal (Kindel and Kennel, 1971). The width of such a layer with anomalous resistivity might be small as compared with the field-aligned scale of low-frequency Alfven waves. Therefore, for the description of wave-layer interaction in such a case the thin layer approximation may be used. This approximation enables one to obtain simpler analytical relationships and to reveal the physical parameters that control this interaction. The problem of Alfven wave interaction with a TL has much in common with the problem of Alfven wave transmission though a layer with a field-aligned potential drop. The first mechanism is caused by local resistivity due to anomalous collisions (Lysak and Carlson, 1981), whereas the latter mechanism is related to the non-resistive potential drop caused by mirror forces in a magnetic flux tube (Lyons, 1980; Vogt

and Haerendel, 1998). The nonlocal dissipation associated with a field-aligned potential drop provides a scale-dependent coupling between the magnetosphere and ionosphere. The magnetospheric flow profile may undergo substantial redistribution during its evolution as a direct consequence of the field-aligned potential drop (Lotko *et al.*, 1987). The studies of Lyons (1980), Vogt and Haerendel (1998), and Vogt (2002) revealed the key spatial parameters of such a coupling mechanism: the resistive scale $\lambda_P$ and $\lambda_A$, determined by the field-aligned conductance of a flux tube, Pedersen conductance of the ionosphere, and Alfven velocity of the magnetosphere. Though the mechanisms of non-resistive field-aligned potential drop and anomalous resistance are physically different, there is a mathematical similarity between these models. Therefore, in this paper we apply for the description of the Alfven wave interaction with a TL with anomalous longitudinal and transverse conductivities an approach similar to the one which has been applied for the consideration of Alfven wave interaction with a plasma layer with non-local Ohm's law for a field-aligned current (Fedorov *et al.*, 2001). The theoretical model developed will be applied to the consideration of the role of Alfven wave damping in turbulent regions that occur in the near-Earth space environment.

## 2. Model of Alfven Wave Interaction with a TL

We consider interaction of Alfven waves with a flat TL with width $h$ and complex transverse $\sigma_\perp$ and field-aligned $\sigma_\parallel$ conductivities. The real parts of these conductivities are caused by the occurrence of effective frequencies of electron, $\nu_e$, and ion, $\nu_i$, collective collisions with turbulent noise. It is assumed that microturbulence is supported by external sources, and is not created by an Alfven wave itself. Otherwise, the wave interaction with a self-generated anomalous resistance layer may be accompanied by a number of specific effects, e.g. limitation of the field-aligned current transmitted by a wave (Mazur *et al.*, 2007).

The model considered here is depicted in Fig. 1. An external straight magnetic field $\mathbf{B}_0$ is normal to the layer, and coincides with the $Z$-axis of an orthogonal coordinate system $\{x,\ y,\ z\}$. The plane $z = 0$ is the interface between the TL ($n = 2$) and lower semi-space ($n = 1$), whereas the plane $z = h$ is the interface with the upper semi-space ($n = 3$). In each plasma layer ($n = 1, 2, 3$) the Alfven velocity $V_{An}$ and wave conductance $\Sigma_{An} = (\mu_0 V_{An})^{-1}$ are constant.

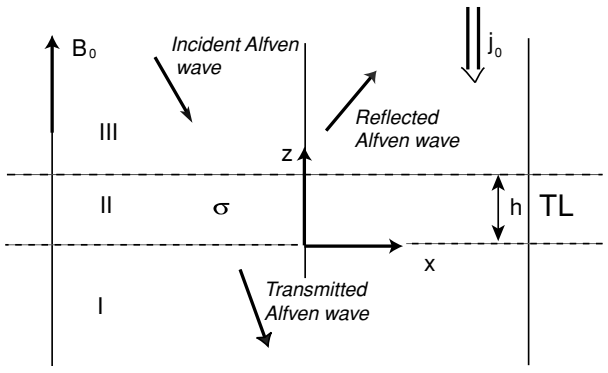


Fig. 1. A sketch of the model of Alfven wave interaction with a turbulent layer (TL).

### 2.1 Alfven waves in a resistive medium

Wave disturbances are presented as a sum of harmonics $\propto \exp(-i\omega t + ik_\perp x)$, where $k_\perp$ is the transverse wave number. From Maxwell's equations and Ohm's law $\mathbf{j} = \hat{\sigma}\mathbf{E}$ the equations for Alfven waves in a medium with transverse $\sigma_\perp(\omega)$ and parallel (field-aligned) $\sigma_\parallel(\omega)$ complex conductivities follow. The possible coupling with the fast compressional mode due to the Hall conductance may be noticeable only for waves with sufficiently large transverse scales, beyond the scales considered here (see estimates in Yagova *et al.* (1999)). In this case Ohm's law becomes

$$\mathbf{j}_\perp = \sigma_\perp \mathbf{E}_\perp\,, \quad \mathbf{j}_\parallel = \sigma_\parallel \mathbf{E}_\parallel \tag{1}$$

Maxwell's equations reduce to

$$\partial_z \begin{pmatrix} E_x \\ B_y \end{pmatrix} = \hat{\mathbf{T}} \begin{pmatrix} E_x \\ B_y \end{pmatrix}, \quad \hat{\mathbf{T}} = \begin{pmatrix} 0 & i\omega - k_\perp^2/\mu_0\sigma_\parallel \\ -\mu_0\sigma_\perp & 0 \end{pmatrix} \tag{2}$$

In a homogeneous medium the coefficients of (2) are coordinate-independent and a dispersion equation can be derived as follows

$$\det\left(\hat{\mathbf{T}} - ik_\parallel \mathbf{1}\right) = 0 \tag{3}$$

where $\mathbf{1}$ is the unit $2 \times 2$ matrix, and $k_\parallel = k_z$ is the field-aligned component of the wave number $\mathbf{k}$. From the dispersion equation (3) we obtain

$$i\omega\mu_0 = \frac{k_\parallel^2}{\sigma_\perp(\omega)} + \frac{k_\perp^2}{\sigma_\parallel(\omega)} \tag{4}$$

Equation (4) makes sense only if the frequency dependence of both conductivities is explicitly indicated.

In the case of resistive MHD one has

$$\mathbf{j}_\perp = \sigma_0\left(\mathbf{E}_\perp + \mathbf{v} \times \mathbf{B}_0\right), \quad \mathbf{j}_\parallel = \sigma_0 \mathbf{E}_\parallel \tag{5}$$

where $\mathbf{v}$ is the plasma velocity. The linearized momentum equation of the MHD system gives

$$\mathbf{v}_\perp = \frac{i\mu_0 V_A^2}{\omega B_0^2}\left(\mathbf{j}_\perp \times \mathbf{B}_0\right) \tag{6}$$

where $V_A$ is the Alfven velocity. Substitution of (6) into (5) provides the possibility to deduce an effective conductivity tensor $\hat{\sigma}(\omega)$ as follows

$$\sigma_\perp^{-1}(\omega) = \sigma_0^{-1} - \frac{\mu_0 V_A^2}{i\omega}\,, \qquad \sigma_\parallel = \sigma_0 \tag{7}$$

In an medium with isotropic conductivity $\sigma_0$ from (4) and (7) the widely used dispersion equation for Alfven waves in a resistive medium follows (Tikhonchuk and Bychenkov, 1995; Senatorov, 1996)

$$\omega^2 - k_\parallel^2 V_A^2 + \left(k_\parallel^2 + k_\perp^2\right)\frac{i\omega}{\mu_0\sigma_0} = 0 \tag{8}$$

However, we believe that a turbulent medium is more adequately modeled as a three-component plasma: electrons,

ions, and plasmons (neutral quasi-particles). We consider neutral quasi-particles as motionless, though at very low frequencies a dragging of plasmons by oscillating ions is possible (Liperovsky and Martjanov, 1973). The transverse conductivity of such a medium is composed of electron and ion conductivities $\sigma_\perp = \sigma_\perp^{(e)} + \sigma_\perp^{(i)}$. Rather complicated relationships for the conductivity tensor can be reduced for low-frequency waves ($\omega \ll \Omega_i$) to the following

$$\sigma_\perp(\omega) \simeq \sigma_P - \frac{i\omega}{\mu_0 \tilde{V}_A^2}, \quad \sigma_\parallel(\omega)^{-1} \simeq \mu_0 \lambda_e^2 (\nu_e - i\omega) \quad (9)$$

The complex transverse conductivity $\sigma_\perp$ is composed of the contributions from the static Pedersen conductivity $\sigma_P$ and polarization current. Here $\tilde{V}_A^2 = V_A^2 \left(1 + r_i^2\right)^2 / \left(1 - r_i^2\right)$ is the Alfven velocity modified by collisions, $\lambda_e = c/\omega_{pe}$ is the plasma electron inertial scale, and $\omega_{pe} = Ne^2/m_e\varepsilon_0$ is the plasma frequency. Further on, for simplicity we neglect the distinction between $V_A$ and $\tilde{V}_A$. Commonly, the contribution of electron inertia in field-aligned conductivity can be omitted, that is,

$$\sigma_\parallel \simeq \sigma_0 = \varepsilon_0 \omega_{pe}^2 \nu_e^{-1} = \left(\mu_0 \lambda_e^2 \nu_e\right)^{-1} \quad (10)$$

Substitution of (9) into (4) results in the generalized dispersion equation for Alfven waves in a turbulent medium

$$k_\parallel^2 = \left(1 + k_\perp^2 \lambda_e^2\right)\left(k_A^2 + i\omega\mu_0\sigma_P\right) - \frac{\sigma_P}{\sigma_0} k_\perp^2 + i \frac{k_A^2 k_\perp^2}{\omega\mu_0\sigma_0} \quad (11)$$

Equation (11) coincides with the equation from Lysak and Dum (1983) in the limiting case $\sigma_P \to 0$. The gas of plasmons is assumed to be like neutral particles upon collisions with electrons and ions in a weakly-collisional plasma. The static field-aligned conductivity (10) is provided by electron collisions, whereas the Pedersen conductivity is supported by ions and electrons, and is determined by the formula

$$\sigma_P = \frac{\omega_{pe}^2 \varepsilon_0}{\Omega_e}\left(\frac{r_e}{1 + r_e^2} + \frac{r_i}{1 + r_i^2}\right) = \sigma_0 \left(\frac{r_e^2}{1 + r_e^2} + \frac{r_e r_i}{1 + r_i^2}\right) \quad (12)$$

where $r_e = \nu_e/\Omega_e$ and $r_i = \nu_i/\Omega_i$ are the parameters which control the frozen-in conditions for electrons and ions, and $\Omega_e$ and $\Omega_i$ are their cyclotron frequencies.

Here we introduce the frequencies

$$\nu_1 = \mu_0 V_A^2 \sigma_P = \frac{\nu_i}{1 + r_i^2} + \frac{m_e}{m_i}\frac{\nu_e}{1 + r_e^2}, \qquad \nu_2 = \frac{k_\perp^2 \lambda_e^2}{1 + k_\perp^2 \lambda_e^2}\nu_e \quad (13)$$

Substituting (13) into (11) transforms the dispersion equation to the following form

$$\frac{k_\parallel^2 V_A^2}{1 + k_\perp^2 \lambda_e^2} = \omega^2 + i\omega(\nu_1 + \nu_2) - \nu_1\nu_2 \quad (14)$$

The wave resistance of the resistive TL is determined by the following relationship:

$$Z_A = \Sigma_A^{-1} = -\frac{ik_\parallel}{\sigma_\perp} \quad (15)$$

In the ideal MHD approximation, when $\sigma_P \to 0$ and $|\sigma_\parallel| \to \infty$, so $\nu_1 \to 0$, $\nu_2 \to 0$, $\lambda_e \to 0$, and the dispersion equation (14) gives $k_\parallel = k_A = \omega/V_A$ and $Z_A = \Sigma_A^{-1} = \mu_0 V_A$. Such a medium may be characterized by the plasma dielectric permeability $\varepsilon_\perp = (c/V_A)^2$. The transverse conductivity is determined by the polarization current $\sigma_\perp = -i\omega/\mu_0 V_A^2$, whereas the field-aligned resistance vanishes.

In the quasi-static case, when $\omega \ll \nu_1\nu_2/(\nu_1 + \nu_2) \leq (\nu_1 + \nu_2)/4$, the first and the second terms in the right-hand side of (14) may be neglected, so this equation describes the attenuation of an electromagnetic field in an anisotropically-conductive medium with the damping scale

$$\kappa = \mathrm{Im}\, k_\parallel \simeq \frac{\sqrt{\nu_1\nu_2}}{V_A} = k_\perp \sqrt{\frac{\sigma_P}{\sigma_0}} \quad (16)$$

We introduce the effective skin-depths, $\delta_\parallel$ and $\delta_P$, determined by the field-aligned and transverse conductivities, correspondingly:

$$\delta_\parallel = \left(1 + k_\perp^2 \lambda_e^2\right)^{-1/2} \sqrt{\frac{2}{\omega\mu_0\sigma_0}}, \qquad \delta_P = \sqrt{\frac{2}{\omega\mu_0\sigma_P}}.$$

When transverse wave numbers and frequencies are not very low, that is $k_\perp \gg (\delta_P \delta_\parallel k_A)^{-1}$ and $k_A \gg \delta_P^{-1}$, or $\nu_1 \ll \nu_2$ and $\nu_1 \ll \omega$, the generalized dispersion equation (14) reduces to the following

$$k_\parallel^2 = \left(1 + k_\perp^2 \lambda_e^2\right) k_A^2 \left(1 + i\frac{\nu_2}{\omega}\right) \quad (17)$$

This equation, with account for (13), may be written as follows

$$\left(1 + k_\perp^2 \lambda_e^2\right)\omega^2 - k_\parallel^2 V_A^2 + k_\perp^2 \frac{i\omega}{\mu_0\sigma_0} = 0 \quad (18)$$

The dispersion equation obtained is somewhat different from the commonly used (8). The longitudinal wave number may be found from the following relationship stemming from (14)

$$k_\parallel = k_A \left(1 + k_\perp^2 \lambda_e^2\right)^{1/2} \left[1 + i\frac{\nu_1 + \nu_2}{\omega} - \frac{\nu_1\nu_2}{\omega^2}\right]^{1/2} \quad (19)$$

Stemming from (19) the damping scale ($k_\parallel = k_A + i\kappa$) of the wave spatial decay upon propagation can be estimated from the following relationship, comprising both field-aligned and transverse resistances

$$\frac{\kappa}{k_A} \simeq \frac{\nu_1 + \nu_2}{2\omega} = \frac{1}{4}(k_\perp \delta_\parallel)^2 + (k_A \delta_P)^{-2} \quad (20)$$

The estimate (20) is valid when $\nu_1 \ll \omega$, and $\nu_2 \ll \omega$. These conditions may be written in the alternative form for the strongly magnetized electrons and ions, i.e. $r_e \ll 1$ and $r_i \ll 1$, and $k_\perp \lambda_e \ll 1$, as follows $\nu_i + (m_e/m_i)\nu_e \ll \omega$, and $k_\perp^2 \lambda_e^2\, \nu_e \ll \omega$.

Further we will see that the critical transverse scales of Alfven wave interaction with TL are much larger than $\lambda_e$, so the correction due to electron inertia may be neglected, $k_\perp \lambda_e \ll 1$.

### 2.2 Alfven waves in a multi-layered system

The field-aligned components $k_\parallel$ of wave vectors in the layers $k_1$, $k_2$, and $k_3$ are determined by relevant dispersion equations. In the upper and bottom semi-planes $k_1 = \omega/V_{A1}$, and $k_3 = \omega/V_{A3}$, whereas the wave number in the TL, $k_2$, is determined by (14) for an Alfven wave in a resistive medium.

In each of the homogeneous layers the solution of Eq. (2) may be presented in the following form:

$$\begin{aligned} B_y &= B_1 e^{-ik_1 z} \\ E_x &= -\mu_0^{-1} Z_{A1} B_1 e^{-ik_1 z} \\ B_y &= B_2 \left(e^{-ik_2 z} + R_2 e^{ik_2 z}\right) \\ E_x &= -\mu_0^{-1} Z_{A2} B_2 \left[e^{-ik_2 z} - R_2 e^{ik_2 z}\right] \\ B_y &= B_3 \left[e^{-ik_3 (z-h)} + R e^{ik_3 (z-h)}\right] \\ E_x &= -\mu_0^{-1} Z_{A3} B_3 \left[e^{-ik_3 (z-h)} - R e^{ik_3 (z-h)}\right] \end{aligned} \tag{21}$$

Here $R$ and $R_2$ are the coefficients of wave reflection from the upper and lower TL boundary, correspondingly, and $B_1$, $B_2$, and $B_3$ are amplitude coefficients.

Each of the plasma semi-spaces ($n = 1, 3$) has a wave resistance $Z_{An} = \Sigma_{An}^{-1} = \pm\mu_0 E_x^{\pm}/B_y^{\pm}$, where the $\pm$ sign corresponds to upward/downward propagating waves. The continuity of the tangential component of the wave electric and magnetic fields at the interface between the layers ($z = 0$) results in the boundary condition

$$E_x = -\mu_0^{-1} Z_{A1} B_y \tag{22}$$

Substitution of (21) into (22) provides a known expression for the coefficient of Alfven wave reflection from a boundary between two plasma layers

$$R_2 = \frac{Z_{A2} - Z_{A1}}{Z_{A2} + Z_{A1}} \tag{23}$$

However, in a multi-layered system a similar formula does not work at the interface $z = h$ and should be modified.

### 2.3 Wave reflection from a finite-width layer

The surface input impedance $Z_{in}$ at the upper boundary of the resistive layer ($z = h$) is determined by the recurrent equations which couple $Z_{in}$ and the impedance at the lower boundary ($z = 0$) as follows

$$Z_{in} = -\mu_0 \frac{E_x}{B_y} = Z_{A2} \frac{Z_{A1} - i Z_{A2} \tan(k_2 h)}{Z_{A2} - i Z_{A1} \tan(k_2 h)} \tag{24}$$

The coefficient $R$ of the Alfven wave reflection from the TL is related to the surface impedance $Z_{in}$ by the known relation

$$R = \frac{Z_{A3} - Z_{in}}{Z_{A3} + Z_{in}} \tag{25}$$

Substituting (24) into (25) we get

$$R = \frac{\Sigma_{A1} - \Sigma_{A3} + \left(\Sigma_{\perp 2} + S k_2^2 h^2\right) G}{\Sigma_{A1} + \Sigma_{A3} + \left(\Sigma_{\perp 2} - S k_2^2 h^2\right) G} \tag{26}$$

Here $\Sigma_{\perp 2} = \sigma_{\perp 2} h$ is the height-integrated transverse conductivity of the resistive layer, such that $\mathrm{Re}\,\Sigma_{\perp 2} = \Sigma_P = \sigma_P h$, and $k_2 h \Sigma_{A2} = i\Sigma_{\perp 2}$. In (26) we have introduced the functions $G(k_2 h) = \tan(k_2 h)/k_2 h$ and $S = \Sigma_{A1}\Sigma_{A3}/\Sigma_{\perp 2}$.

Now we find the coefficient of wave transmission through the layer. From the continuity of magnetic field at $z = h$ and $z = 0$ it follows that

$$\frac{B_2}{B_3} = \frac{1 + R}{\exp(-ik_2 h) + R_2 \exp(ik_2 h)}, \tag{27}$$

$$\frac{B_1}{B_2} = 1 + R_2 \tag{28}$$

Combining (27), the transmission coefficient $T = B_1/B_3$ can be found. Substituting in (27) the relationships (23) and (25) for the reflection coefficients $R_2$ and $R$, we get after simple algebra

$$T = \frac{2}{\cos k_2 h} \times \frac{\Sigma_{A1}}{\Sigma_{A1} + \Sigma_{A3} + \left(\Sigma_{\perp 2} - S k_2^2 h^2\right) G} \tag{29}$$

### 2.4 Wave reflection from a thin layer

We define a TL as an "optically thin" (or just thin) layer when $|k_2 h| \ll 1$. This condition can be more explicitly expressed in two cases. For large transverse wave numbers, satisfying the inequality $(\nu_1 + \nu_2) \gg \omega$, from (11) the approximate relation (16) follows. Then, the condition of a thin layer has the form

$$|k_\perp \lambda_P| \ll 1 \tag{30}$$

Here we have introduced the dissipative scale $\lambda_P = \sqrt{\left|\frac{\sigma_{\perp 2}}{\sigma_\parallel}\right|} h = \sqrt{|Q\Sigma_{\perp 2}|}$, where $Q = h/\sigma_0$ is the field-aligned integrated resistance of the layer.

When transverse wave numbers are so small that $\nu_2 \ll \nu_1$ and $\nu_2 \ll \omega$, the condition of the thin layer approximation is somewhat different. In this case the wave dispersion equation in a TL gives $k_2^2 \simeq i\omega\mu_0\sigma_\perp$. For low-frequency waves with $\omega \ll \nu_1$ we have $\sigma_\perp \simeq \sigma_P$. As a result, a TL may be considered as "thin" when

$$h \ll \delta_P \tag{31}$$

In this limit of large-scale disturbances ($k_\perp \to 0$) the reflection and transmission coefficients are weakly dependent on the transverse wave numbers, and are as follows

$$R \simeq R_0 = \frac{1 - \overline{\Sigma}_{A3}}{1 + \overline{\Sigma}_{A3}} \qquad T \simeq T_0 = \frac{2\overline{\Sigma}_{A1}}{1 + \overline{\Sigma}_{A3}} \tag{32}$$

Here we have introduced the normalized Alfven conductances

$$\overline{\Sigma}_{A1} = \frac{\Sigma_{A1}}{\Sigma_{A1} + \Sigma_{\perp 2}} \qquad \overline{\Sigma}_{A3} = \frac{\Sigma_{A3}}{\Sigma_{A1} + \Sigma_{\perp 2}}$$

When the condition (30) of the thin layer approximation is valid, the coefficient of wave reflection from a layer (26) reduces to the following

$$R \simeq R_0 \frac{1 - q_P \overline{k}_\perp^2}{1 + q_m \overline{k}_\perp^2} \tag{33}$$

where

$$q_P = \frac{\overline{\Sigma}_{A1}}{1 - \overline{\Sigma}_{A3}} \left(1 + \frac{1}{3} \frac{\Sigma_{\perp 2}^2}{\Sigma_{A1}\Sigma_{A3}}\right) \tag{34}$$

$$q_{\rm m} = \frac{\overline{\Sigma}_{\rm A1}}{1+\overline{\Sigma}_{\rm A3}}\left(1-\frac{1}{3}\frac{\Sigma_{\perp 2}^2}{\Sigma_{\rm A1}\Sigma_{\rm A3}}\right) \tag{35}$$

In (33) the dimensionless transverse wave number $\overline{k}_\perp = k_\perp \lambda_{\rm A}$ has been introduced.

The parameter $\lambda_{\rm A} = (\Sigma_{\rm A3} Q)^{1/2}$ is determined by the altitude-integrated field-aligned resistance $Q$ and the Alfven velocity above the TL. According to its physical sense, this parameter is the transverse scale when the field-aligned column resistance matches the Alfven wave resistance $\Sigma_{\rm A}^{-1}$. The previously introduced parameter, the resistive length $\lambda_{\rm P}$, is the transverse wave scale when the scale of wave penetration into a TL with conductivity $\sigma_\parallel$ matches the layer width $h$. As one will see further, the key parameter of the Alfven wave interaction with a thin TL is the ratio between $\lambda_{\rm A}$ and the wave transverse scale, namely $k_\perp \lambda_{\rm A}$. At the same time, the ratio between the parameter $\lambda_{\rm P}$ and $k_\perp^{-1}$ more adequately characterizes the wave dissipation in a thin TL. These two parameters, $\lambda_{\rm P}$ and $\lambda_{\rm A}$, were first introduced as the resistive scale (Lyons, 1980) and transient length scale (Vogt and Haerendel, 1998; Vogt, 2002) of magnetosphere-ionosphere coupling, in studies of the mathematically similar problem of the Alfven wave interaction with the non-resistive potential drop region.

From (33) it follows that if the Alfven wave transverse scale $k_\perp^{-1}$ matches the critical value

$$L_\perp^* = \lambda_{\rm A}\left[\frac{1+\Sigma_{\perp 2}^2/3\Sigma_{\rm A1}\Sigma_{\rm A3}}{1+(\Sigma_{\perp 2}-\Sigma_{\rm A3})/\Sigma_{\rm A1}}\right]^{1/2} \tag{36}$$

then, while $L_\perp^* \geq \lambda_{\rm P}$, the input impedance $Z_{\rm in}$ equals the Alfven wave resistance $\Sigma_{\rm A3}$, and the reflection coefficient from a thin TL vanishes, $R = 0$. Thus, the dependence $R\left(\overline{k}_\perp\right)$ (33) should change sign at the critical $k_\perp^* = 1/L_\perp^*$.

Now we find the coefficient of the wave transmission through a thin layer. Decomposing $\cos(k_2 h)$ and $G(k_2 h)$ into Taylor series, and neglecting in (29) terms of the order of $(k_2 h)^3$, we obtain

$$T \simeq T_0\left(1+\frac{1}{2}q_{\rm T}\overline{k}_\perp^2\right)^{-1} \tag{37}$$

where

$$q_{\rm T} = \frac{\Sigma_{\perp 2}}{\Sigma_{\rm A3}}\left(1-\frac{2}{3}\frac{\Sigma_{\perp 2}}{\Sigma_{\rm A1}+\Sigma_{\rm A2}+\Sigma_{\rm A3}}\right)+T_0$$

### 2.5 Alfven wave energy losses in a TL

Let $S^{(\rm i)}$, $S^{(\rm r)}$, and $S^{(\rm t)}$ be densities of the energy fluxes carried by incident, reflected, and transmitted waves, respectively. The energy losses of Alfven waves in a resistive layer are determined as follows

$$J = S^{(\rm i)} - S^{(\rm r)} - S^{(\rm t)} \tag{38}$$

The energy flux densities in incident, reflected, and transmitted Alfven waves may be presented via the amplitude of Alfven waves in the magnetosphere $B_3$ as follows

$$S^{(\rm i)} = \frac{V_{\rm A3}}{2\mu_0}|B_3|^2 \quad S^{(\rm r)} = \frac{V_{\rm A3}}{2\mu_0}|RB_3|^2 \quad S^{(\rm t)} = \frac{V_{\rm A1}}{2\mu_0}|TB_3|^2 \tag{39}$$

The energy loss $\alpha$ in a TL, normalized to the energy flux of incident waves, can be found from (38) and (39)

$$\alpha = \frac{J}{S^{(\rm i)}} = 1-|R|^2-\frac{V_{\rm A1}}{V_{\rm A3}}|T|^2 \tag{40}$$

**2.5.1 Finite-width TL** In a finite-width TL with thickness $h$ the energy absorption rate comprises two terms $q_\perp$ and $q_\parallel$, where

$$q_\perp = \frac{1}{2}\int_0^h \sigma_{\rm P}|E_x|^2\,dz \qquad q_\parallel = \frac{1}{2}\int_0^h \sigma_0\left|\frac{j_z}{\sigma_\parallel}\right|^2 dz \tag{41}$$

From (21) we have

$$E_x = -\frac{Z_{\rm A2}B_2}{\mu_0}\left(e^{-ik_2 z}-R_2 e^{ik_2 z}\right),$$
$$j_z = \frac{ik_\perp}{\mu_0}B_2\left(e^{-ik_2 z}+R_2 e^{ik_2 z}\right) \tag{42}$$

where $B_2$ and $B_3$ are related by (27). Substituting (42) into (41), and taking into account (40), we obtain the relationship for the normalized energy loss due to the transverse and field-aligned conductivities, as follows

$$\alpha_\perp = \frac{q_\perp}{S^{(\rm i)}} = \frac{\Sigma_{\rm P}\Sigma_{\rm A3}}{|\Sigma_{A2}|^2}KI_1 \qquad \alpha_\parallel = \frac{q_\parallel}{S^{(\rm i)}} = \overline{k}_\perp^2 KI_2 \tag{43}$$

The coefficients $K(k_2 h)$ and $I_{1,2}(k_2 h)$ in (43) are as follows

$$K = \left|\frac{1+R}{\exp(-ik_2 h)+R_2\exp(ik_2 h)}\right|^2 \tag{44}$$

$$I_{1,2} = E_0\left(2{\rm Im}(k_2 h)\right)+|R_2|^2 E_0\left(-2{\rm Im}(k_2 h)\right) \mp 2{\rm Re}\left(R_2 E_0(2i{\rm Re}(k_2 h))\right) \tag{45}$$

where the function $E_0$ is $E_0(z) = z^{-1}(\exp z - 1)$. The relationship for $K$ can be transformed, using (26), into the following

$$K = \left|\frac{\Sigma_{\rm A1}+\Sigma_{\rm A2}}{\cos k_2 h\left[\Sigma_{\rm A1}+\Sigma_{\rm A3}+\left(\Sigma_{\perp 2}-Sk_2^2 h^2\right)G\right]}\right|^2 \tag{46}$$

**2.5.2 Thin TL** In the thin layer approximation modified expressions for coefficients $I_{1,2}(k_2 h)$ and $K(k_2 h)$ may be found in Fedorov *et al.* (2007). Using them, from (43) it is possible to find the "transverse" and "field-aligned" energy losses in the thin layer approximation

$$\alpha_\perp = \alpha_{\perp 0}\left\{1+\frac{\Sigma_{\rm A1}}{\Sigma_{\rm A3}}\left(1+\frac{1}{3}\frac{\Sigma_{\rm P}}{\Sigma_{\rm A1}}\right)\overline{k}_\perp^2 + \frac{1}{3}\left(\frac{\Sigma_{\rm A1}}{\Sigma_{\rm A3}}\right)^2\overline{k}_\perp^4\right\}\Delta^{-1} \tag{47}$$

$$\alpha_\parallel = \alpha_{\parallel 0}\overline{k}_\perp^2\left\{1+\frac{\Sigma_{\perp 2}}{\Sigma_{\rm A1}}+\frac{1}{3}\left(\frac{\Sigma_{\perp 2}}{\Sigma_{\rm A1}}\right)^2 + \frac{1}{3}\frac{\Sigma_{\perp 2}}{\Sigma_{\rm A3}}\overline{k}_\perp^2\right\}\Delta^{-1} \tag{48}$$

where

$$\Delta\left(\overline{k}_\perp^2\right) = \left|1+\frac{1}{2}\frac{\Sigma_{\perp 2}}{\Sigma_{\rm A3}}\overline{k}_\perp^2\right|^2\left|1+q_{\rm m}\overline{k}_\perp^2-\frac{1}{3}\frac{\Sigma_{\rm A1}\Sigma_{\perp 2}}{\Sigma_{\rm A3}\Sigma_{\rm T}}\overline{k}_\perp^4\right|^2$$
$$\Sigma_{\rm T} = \Sigma_{\rm A1}+\Sigma_{\perp 2}+\Sigma_{\rm A3}$$

Coefficients $\alpha_{\perp 0}$ and $\alpha_{\parallel 0}$ in (47) determine the energy losses for waves with large scales, when $\overline{k}_\perp \to 0$, and are as follows

$$\alpha_{\perp 0} = \frac{4\Sigma_P \Sigma_{A3}}{|\Sigma_T|^2}, \qquad \alpha_{\parallel 0} = \frac{4\Sigma_{A1}^2}{|\Sigma_T|^2} \tag{49}$$

## 3. Numerical and Analytical Estimates

Here we provide the results of both numerical calculations with the exact formula and estimates using the thin layer approximation for several models, based on published parameters of near-Earth space and turbulence.

### 3.1 Models of a TL

To validate the significance of the effects considered here we provide numerical results for some models of anomalous conductivity presented in the literature. To highlight the effect of anomalous resistance in a layer, we make the Alfven velocity the same at all altitudes. This way we exclude an additional wave reflection at $V_A$ jumps.

The effective frequency of particle-plasmon collisions in general is a function of the turbulence spectral power $W$ and plasma parameters. Estimating this frequency is a difficult problem, which should be solved separately for each particular turbulence type. Precise estimates demand knowledge of turbulence type, its spatial spectra, dominating non-linear saturation mechanism, etc. Many of these parameters are not easily observable, so the estimates provided in the literature vary over a wide range. Assuming that collision frequencies are known from the solution of a relevant kinetic problem, one may use the developed relationships to validate the Alfven wave transmission through a particular TL. For that, one has to replace in the plasma conductivities (10) and (12) the frequencies of collision of charged particles with neutrals by the collective particle-plasmon collision frequencies.

For ion-acoustic turbulence an estimate of the maximal collision frequencies has been shown (Liperovsky and Pudovkin, 1983) to be

$$\nu_e \simeq \omega_{pe}(W/nT), \qquad \nu_i \simeq \omega_{pi}(W/nT)^2 \tag{50}$$

where $W/nT$ is the ratio between the energy densities of turbulent noise and background plasma. However, the ion-acoustic turbulence can exist in a highly non-isothermal plasma only when $T_e \gg T_i$. In other situations the electrostatic ion-cyclotron instability dominates. This instability saturates at a level which provides $\nu_e = (0.2 - 1)\Omega_i$ (Ionson, 1976; Hudson *et al.*, 1978).

The interaction of Alfven waves (period $T = 100$ s) with a TL has been calculated for several models with different types of turbulence. The parameters of the background plasma have been chosen to correspond to typical values in the auroral cavity of the upper ionosphere: $N = 10^3$ cm$^{-3}$, $B = 1.45 \cdot 10^3$ nT. These values correspond to Alfven velocities $V_{A1} = V_{A2} = 10^3$ km/s, and wave conductance $\Sigma_A = 0.8$ Ohm$^{-1}$. Characteristic frequencies in such plasma are $\omega_{pe} \simeq 1.79 \cdot 10^6$ s$^{-1}$, $\omega_{pi} \simeq 4.17 \cdot 10^4$ s$^{-1}$, $\Omega_e \simeq 2.55 \cdot 10^5$ s$^{-1}$, and $\Omega_i \simeq 1.39 \cdot 10^2$ s$^{-1}$. The electron inertial scale is $\lambda_e \simeq 170$ m.

To validate the thin layer approximation we have made calculations for two model layers with parameters adapted from (Trakhtenhertz and Feldstein, 1985):

**TF-1:** $h = 30$ km, $\nu_e = 10^3$ s$^{-1}$, $\nu_i = \sqrt{m_e/m_i}\nu_e = 23$ s$^{-1}$;

**TF-2:** $h = 100$ km, $\nu_e = 10^2$ s$^{-1}$, $\nu_i = \sqrt{m_e/m_i}\nu_e = 2.3$ s$^{-1}$.

For the TF-1 and TF-2 models the anomalous field-aligned conductivities $\sigma_0 = 2.8 \times 10^{-2}$ Ohm$^{-1} \cdot$ m$^{-1}$ and $2.8 \times 10^{-1}$ Ohm$^{-1} \cdot$ m$^{-1}$, resistances $Q = h/\sigma_\parallel \simeq 10^6$ Ohm $\cdot$ m$^2$ and $0.35 \times 10^6$ Ohm $\cdot$ m$^2$, respectively. The Pedersen conductivity $\sigma_P = 1.8 \cdot 10^{-5}$ Ohm$^{-1} \cdot$ m$^{-1}$ and $0.19 \cdot 10^{-5}$ Ohm$^{-1} \cdot$ m$^{-1}$, Pedersen conductances $\Sigma_P = 0.55$ Ohm$^{-1}$ and $0.19$ Ohm$^{-1}$, the Alfven resistive scales $\lambda_A \simeq 0.9$ km and 0.5 km, dissipative scales $\lambda_P \simeq 0.76$ km and 0.26 km, respectively.

Further, the absorption of Alfven waves in a TL has been calculated for two characteristic types of high-frequency plasma turbulence:

**Model S**: A layer with ion-acoustic turbulence. Anomalous collision frequencies are estimated from the relationship of weak turbulence theory (50) assuming $W/nT \simeq 10^{-3}$, and $h = 10^3$ km. A feature of this model is a strong contrast ($\sim 4 \cdot 10^4$) between the electron $\nu_e$ and ion $\nu_i$ collision frequencies.

**Model C**: A layer with ion-cyclotron turbulence. Anomalous collision frequencies are estimated as $\nu_e \simeq 0.7\Omega_i$, $\nu_i = 0.1\nu_e$, and $h = 10^3$ km. In this model the electron and ion collision frequencies differ by only an order of magnitude.

### 3.2 Reflection and transmission coefficients

The dependence of the reflection coefficient $R$ on normalized transverse wave number $k_\perp \lambda_A$ with account of both conductivities is shown in Fig. 2. Here and further the calculations made with the exact formula are denoted by solid lines, and calculations in the thin layer approximation are shown by dotted lines. The model code is indicated near appropriate curves.

The most prominent feature of the reflection coefficient is the change of its sign at certain $\overline{k}_\perp \sim 0.2$–$0.8$, depending on the model. The vertical dashed lines denote the values $k_\perp^* =$

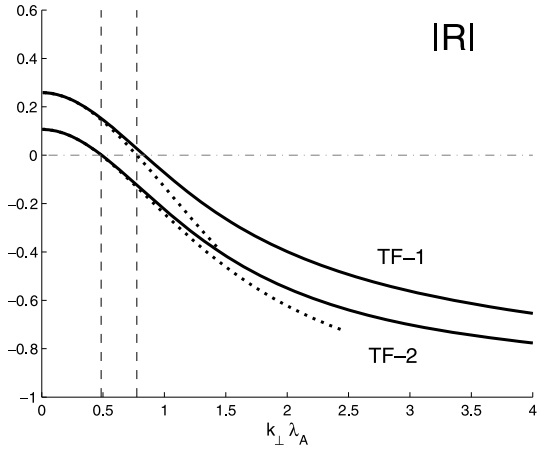


Fig. 2. The dependence of the reflection coefficient $R$ on normalized transverse wave number $k_\perp \lambda_A$ with account of both transverse and field-aligned conductivities for the TF-1 and TF-2 models. Solid lines correspond to exact relationships, whereas dashed lines denote the thin layer approximation. Vertical dotted lines denote the critical values of transverse wave numbers $k_\perp^* = 1/L_\perp^*$.

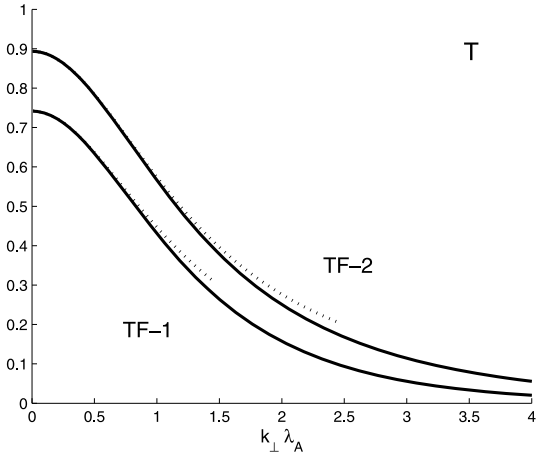


Fig. 3. The scale dependence of the transmission coefficient $T(k_\perp \lambda_A)$ according to exact (solid lines) and approximate (dashed lines) relationships for the TF-1 and TF-2 models.

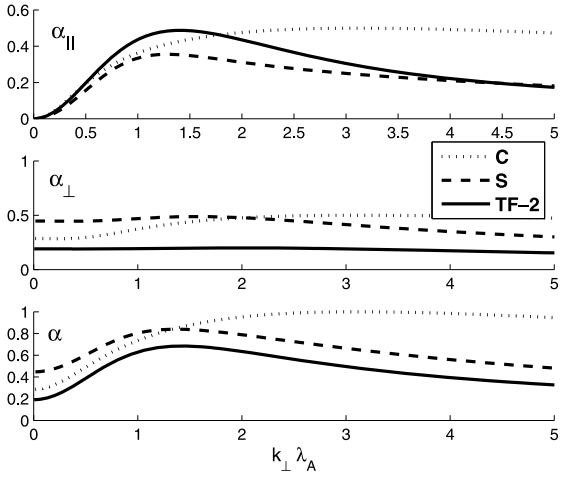


Fig. 4. Dependence of energy losses due to the field-aligned $\alpha_\parallel$, transverse $\alpha_\perp$, and total $\alpha$ TL resistance on the normalized transverse wave number $k_\perp$ for the TF-2, S, and C models.

$1/L_\perp^*$ which correspond to critical scales when $R$ should change sign in the thin layer approximation according to (36). For the models TF-1 and TF-2 the condition $L_\perp^* \geq \lambda_P$ is valid, and the relationship (36) gives a correct estimate of such critical $k_\perp$. Large-scale Alfven waves ($k_\perp \to 0$) reflect from a resistive layer as from a conductor $R > 0$, whereas small-scale waves ($k_\perp \to \infty$) reflect as from an insulator, that is $R \to -1$ when $k_\perp \gg \lambda_P^{-1}$. Thus, both large-scale and small-scale waves effectively reflect from a TL.

Figure 3 shows the dependence of the transmission coefficient $T$ on $k_\perp \lambda_A$. The coefficient $T$ decreases monotonically with increase of $k_\perp$ from $T_0$ at $k_\perp = 0$, and further approaches exponentially 0 as $k_\perp \lambda_P \to \infty$. Indeed, from (29) for large $k_\perp \lambda_P$ the asymptotic estimate follows $T \simeq 4(\Sigma_P/\Sigma_{A3})(k_\perp \lambda_P)^{-1} \exp(-k_\perp \lambda_P)$. Thus, at large $k_\perp$ the energy of incident waves nearly totally converts into the energy of reflected waves.

The comparison of calculation results in the thin layer approximation (dotted lines in Figs. 2–3) and with the complete formula for a finite width layer (solid lines) shows that the approximation works well at scales $k_\perp \lambda_A \leq 1$ for both models.

### 3.3 Energy losses in a TL

The dependence of energy losses in a layer with anomalous conductivity on the transverse wave number for models TF-2, S, and C is shown in Fig. 4. Separate energy losses due to field-aligned $\alpha_\parallel$ and transverse $\alpha_\perp$ conductivities have been calculated from (43). The total energy losses $\alpha$ have been calculated using formula (40), in which the exact coefficients of reflection and transmission are determined from (26, 29), and the coefficients in the thin layer approximation are derived from (33, 37).

For all TL models considered the energy losses are maximal at wave scales $k_\perp \sim \lambda_A^{-1}$. The part of energy losses $\alpha_\perp(\overline{k}_\perp)$ due to transverse resistance weakly depends on the wave scale (middle panel in Fig. 4). In contrast, the part $\alpha_\parallel(\overline{k}_\perp)$ reaches peak values at $\overline{k}_\perp \simeq 1.4$ (upper panel in Fig. 4). This peak is responsible for the maximum occurrence in the dependence of total energy losses on wave numbers $\alpha(\overline{k}_\perp)$ (bottom panel).

Thus, wave energy losses are determined by the transverse resistance for large-scale disturbances, $k_\perp \lambda_A \ll 1$. For small-scale disturbances $k_\perp \lambda_A \gg 1$ both mechanisms contribute at a similar rate. For intermediate wave scales, $k_\perp \sim \lambda_A^{-1}$, the energy losses are mostly determined by the field-aligned resistance.

## 4. Geophysical Consequences

### 4.1 Pc1 waves in the vicinity of the dayside cusp

Many studies have proposed the cusp region as a likely source of some of the Pc1-2 waves observed at high latitudes on the ground. Intense broadband wave activity in the Pc1-2 band is often reported by low- and mid-altitude satellites (e.g., Erlandson *et al.*, 1988). Polar satellite observations (Le *et al.*, 2001) showed that narrowband waves at frequencies ~0.2–3 Hz are a permanent feature in the vicinity of the polar cusp. These waves have been found in the magnetosphere adjacent to the cusp (both poleward and equatorward of the cusp) and in the cusp itself. The occurrence of waves is coincident with the magnetic field depression associated with enhanced plasma density indicating the entry of the magnetosheath plasma into the cusp, which suggests that the waves are generated in this region by the precipitating magnetosheath plasma. The polarization and propagation angles of the waves are highly variable, whereas energy flux is mostly guided along the background magnetic field. The wave frequencies are generally controlled by the local $B_0$ strength, which strongly suggests that these waves are generated locally and absorbed in the near vicinity of the generation region.

However, analysis of several years' data from the MACCS ground magnetometer array repeatedly failed to find any Pc1-2 signatures when satellites and/or radars reported that the cusp was overhead of a given MACCS station. This puzzle led Dyrud *et al.* (1997) to undertake a study of the latitudinal patterns seen in Pc1-2 data obtained by the MACCS array, which suggested that the high-latitude, unstructured Pc1-2 in fact originated in the high latitude plasma mantle, not the cusp. Later on, Engebretson *et al.* (2005) reported on simultaneous field and parti-

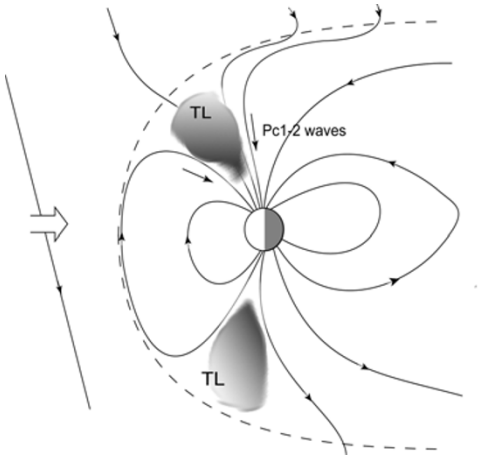


Fig. 5. Sketch of possible Pc1-2 wave propagation paths in the vicinity of the cusp. The cusp proper has been depicted as a TL.

cle observations from the Polar satellite and from ground magnetometers that confirm the presence of the "mantle" waves and characterize the ion distributions associated with them. In-situ particle observations appear to confirm the generation mechanism suggested by Dyrud *et al.* (1997), that cusp particles mirroring at low altitudes and then traveling outward in the plasma mantle poleward of the cusp are the source of the free energy for these waves. The Polar particle data showed upward ion fluxes coincident with each mantle wave intensification, and in association with a downward Poynting vector. In contrast, the Poynting vector associated with the intense, broadband ULF activity in the cusp shows mixed direction. This is consistent with the apparent lack of a "cusp signature" in ground magnetometer observations in the Pc1-2 frequency range.

The inability of Pc1-2 waves to propagate through the cusp region may be related to enhanced wave absorption in highly turbulent cusp plasma, as illustrated in Fig. 5. Observations on OGO-5 (Fredericks *et al.*, 1973) showed that the low altitude cusp (altitudes from $1R_e$ to $3.2R_e$) is filled with intense ($\langle E \rangle \simeq 9 \times 10^{-2}$ V/m) high-frequency electrostatic turbulence. The mechanism of this turbulence is probably ion-acoustic or Bunemann instabilities driven by intense field-aligned current (typically, $j_\parallel \simeq 2 \times 10^{-5}$ A/m$^2$) inside the cusp. This turbulence should provide anomalous collisionless resistivity, where the frequency of effective collisions of electrons with electrostatic modes can be estimated from (50). For the above parameters, the collisionless resistivity in the low-altitude cusp is $\rho \simeq 8$ Ohm·m, which produces a field-aligned potential drop at a distance along a field line $S \simeq 1.3 \times 10^7$ m of as much as $\Delta\Phi \simeq j_\parallel \rho S \simeq 2$ kV.

For qualitative estimates the relationship (20) from the theory of Alfven wave propagation via a turbulent infinite homogeneous medium can be applied. To model the mid-altitude cusp we assume the following plasma and wave parameters: $f = 1$ Hz, $V_A = 10^3$ km/s with $N = 10^3$ cm$^{-1}$ and $B_0 = 1.4 \times 10^3$ nT. The corresponding characteristic plasma frequencies and scales are $\Omega_e \simeq 2.6 \times 10^5$ s$^{-1}$, $\omega_{pe} \simeq 1.8 \times 10^6$ s$^{-1}$, and $\lambda_e \simeq 170$ m. The measured anomalous field-aligned resistivity $\rho_0 = 8$ Ohm$^{-1} \cdot$ m$^{-1}$ should correspond to an electron collision frequency $\nu_e = \rho_0 / \left(\mu_0 \lambda_e^2\right) \simeq 2.3 \cdot 10^2$ s$^{-1}$. Assuming that anomalous collisions are similar to charged particle collisions with neutral particles, one may suppose that $\nu_i = \sqrt{m_e/m_i}\nu_e \simeq 5.3$ s$^{-1}$. From these estimates it follows that $\sigma_P \simeq 4.3 \times 10^{-6}$ Ohm$^{-1} \cdot$ m$^{-1}$, and $\delta_P \simeq 240$ km. The expected spatial damping rate is $\kappa \simeq 0.25 \cdot 10^{-2}$ km$^{-1}$, and $k_A/\kappa \simeq 2.5$, thus indicating that the amplitude of such waves should decrease by a factor of $e$ in a distance of about 0.4 wavelengths. The damping owing to field-aligned resistance is small, $k_A/\kappa \simeq 10^4$, for transverse wave scales $k_\perp^{-1} \sim 10^2$ km, and the main contribution is provided by the transverse resistivity.

Our model thus predicts that the occurrence of electrostatic turbulence in the cusp causes substantial damping of Alfven waves in the cusp, consistent with the Pc1-2 observational studies reviewed above. Surely, alternative wave absorption mechanisms also might be operative in the cusp region, such as Landau damping due to the resonant wave-particle interaction in the high beta plasma of the cusp, but their consideration is beyond the topic of this paper. These mechanisms may be especially important when the damping due to the anomalous resistance become ineffective, e.g. for a large transverse wave scales.

### 4.2 Observations of nonlinear damping of Pi2 pulsations

According to the traditional point of view, Pi2 pulsations are transient oscillatory processes stimulated by substorm onset. Therefore, Pi2 waveforms are commonly modeled with a linear damped oscillatory function $\propto \exp(-\gamma t)\cos(\omega t + \varphi)$, where the frequency $\omega$ is the eigenfrequency of field line oscillations, and the damping rate $\gamma$ is determined by the dissipation in the night side ionosphere. However, "classical" oscillations of this kind are very rare, and may be observed at low or middle latitudes only. At auroral latitudes, Pi2 bursts have complicated waveforms indicating that they are composed of contributions from several nearly simultaneous sources.

We'd like to notice that linear damping as predicted by modeling an exponential function is very rarely observed. Among the large variety of observed wave forms the following kind may be selected—a rapid damping of the intense part of a signal and a slower damping of the weaker part of a signal. Examples of such non-linear Pi2 damping detected on the IMAGE array on Sep. 25, 2001 are shown in Fig. 6. This example shows that small-amplitude Pi2 damp gradually, while the intense Pi2 pulse damps much faster, right after the first excursion. By and large, this kind of a signal looks like the stalling of an oscillatory process under large amplitude conditions. In other words, the magnetospheric Alfven resonator (MAR) turns out to be highly over-damped under large amplitude Pi2 conditions.

There is other observational evidence of the occurrence of non-linear Pi2 damping. Earlier studies of Pi2 damping rate during substorms (Barsukov and Pudovkin, 1970; Gudkova *et al.*, 1973) found that the damping rate increases if the magnitude of accompanying magnetic bays $\Delta H$ is larger than some critical value ~100 nT. The dependence of the normalized damping rate on substorm magnetic disturbance (Gudkova *et al.*, 1974) indicated that during intense

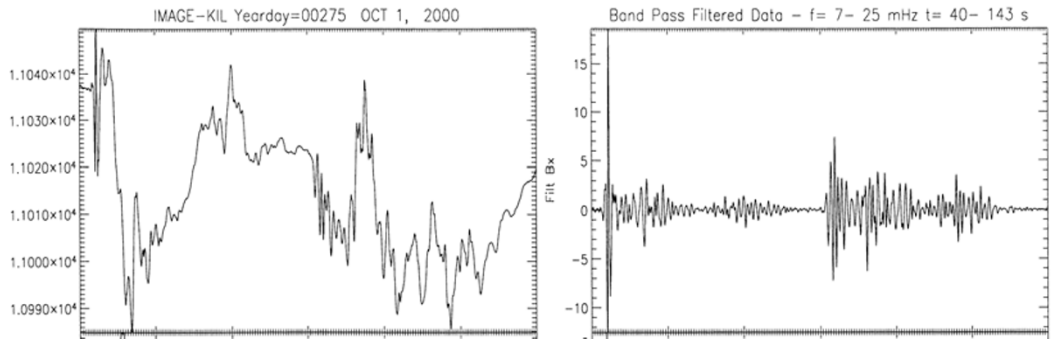


Fig. 6. Examples of Pi2 signals ($H$ component) with a sudden drop of amplitude, recorded at Kilpisjarvi, a station of the IMAGE array, on 10/01/2001 (day 275), 20–23 UT: raw data (left panel), and band-filtered 7–25 mHz magnetogram (right-hand panel).

magnetic disturbances the Pi2 damping rate acquired an additional component $\gamma^*$, such that $\gamma \to \gamma + \gamma^*$. It was supposed that this additional non-linear damping mechanism is related to the onset of plasma turbulence and anomalous collisions, when magnetospheric field-aligned currents exceed thresholds necessary for the excitation of anomalous resistance (Shalimov and Liperovsky, 1988). Here is a simple estimate to justify this assumption.

Using a schematic model of an auroral electrojet driven by field-aligned currents at its boundaries (Swift, 1981), one can relate the magnitude of a ground magnetic disturbance $\Delta B$ to the value of a field-aligned magnetospheric current. The ground magnetic disturbance is produced by a band of Hall current with surface density $i_{\rm H}$ and width $d$ located at altitude $h$ above the ground is as follows

$$\Delta B = \begin{cases} \dfrac{\mu_0 i_{\rm H}}{2} & \text{at} \quad d \geq h, \\ \dfrac{\mu_0 i_{\rm H} d}{2\pi h} & \text{at} \quad d \ll h. \end{cases} \tag{51}$$

Above a highly-conductive Earth's crust these values are to be doubled. The ionospheric current is related to the field-aligned current above the ionosphere by the current continuity condition. Taking into account a scale factor $B^{(\rm m)}/B^{(\rm i)}$ owing to altitude variations of the flux tube cross-section, we obtain an estimate of the magnetospheric field-aligned current density

$$j_{\parallel}^{(\rm m)} = \frac{B^{(\rm m)}}{B^{(\rm i)}} \frac{\Sigma_{\rm P}}{\Sigma_{\rm H}} \frac{i_{\rm H}}{d} \tag{52}$$

Using 51 for auroral electrojet with $d = 10$ km, $h = 10^2$ km, and $\Sigma_{\rm H}/\Sigma_{\rm P} = 10/\pi$, we obtain for altitude $\sim 2R_{\rm E}$ ($B^{(\rm m)}/B^{(\rm i)} \simeq 0.1$) for a magnetic disturbance $10^2$ nT above a highly-conductive crust the estimate of the magnetospheric current $j^{(\rm m)} \simeq 7.5 \times 10^{-6}$ A/m$^2$. This estimated value is about the critical current magnitude necessary for the excitation of ion-acoustic or ion-cyclotron instabilities in the upper ionosphere (assuming $N = 10^3$ cm$^{-3}$).

### 4.3 Estimate of the $Q$-factor of the MAR with TL

Let us augment the TL model considered in Section 2 above (Fig. 1) by the occurrence of the ionosphere in the plane $z = -h_1$ with Pedersen conductance $\Sigma_{\rm IP}$. Then, at $z = -h_1$ we have a boundary condition for Alfven waves

$$E_x = -(\mu_0 \Sigma_{\rm IP})^{-1} B_y \tag{53}$$

Re-calculating the impedance from the ionospheric layer ($z = -h_1 + 0$) to the bottom boundary of TL ($z = 0 - 0$) we obtain the boundary condition:

$$E_x = -(\mu_0 \Sigma_1)^{-1} B_y \qquad \Sigma_1 = \Sigma_{\rm A1} \frac{\overline{\Sigma}_{\rm IP} - i \tan k_1 h_1}{1 - i \overline{\Sigma}_{\rm IP} \tan k_1 h_1} \tag{54}$$

where $\overline{\Sigma}_{\rm IP} = \Sigma_{\rm IP}/\Sigma_{\rm A1}$ is the normalized ionospheric conductance.

Substitution in (22) instead of the wave conductance $\Sigma_{\rm A1}$ the $\Sigma_1$ from (54), results in the coefficient of Alfven wave reflection from the combined system TL + ionosphere

$$R = \frac{\Sigma_1 - \Sigma_{\rm A3} + \left(\Sigma_{\perp 2} + S k_2^2 h^2\right) G}{\Sigma_1 + \Sigma_{\rm A3} + \left(\Sigma_{\perp 2} - S k_2^2 h^2\right) G} \tag{55}$$

When TL are absent, the relation (55) reduces to the known formula for the coefficient of Alfven wave reflection from the ionosphere (Scholer, 1970; Maltsev, 1977)

$$R_{\rm I} = \frac{\overline{\Sigma}_{\rm IP} - 1}{\overline{\Sigma}_{\rm IP} + 1} \tag{56}$$

Now we use these results for the consideration of a MAR with symmetric thin TLs above the northern and southern ionospheres. Let an Alfven impulse with amplitude $b_0$ impinge on one of the ionospheres, as illustrated in Fig. 7. Upon interaction with this ionosphere a part of impulse energy, $Tb_0$, transmits through the ionosphere, and a part, $b_1 = Rb_0$, is reflected. After a second interaction with the conjugate ionosphere the relevant parts are $R^2 b_0$ and $TR^2 b_0$, etc. The resulting damping rate and $Q$-factor of the MAR with a TL can be estimated as

$$\gamma = -\frac{\omega}{2\pi} \ln |R|^2 \qquad Q = \frac{\omega}{2\gamma} = -\frac{\pi}{2 \ln |R|} \tag{57}$$

where $R$ is determined by (55).

Figure 8 shows a comparison of the results of numerical calculations of the coefficient of reflection from the ionosphere (dashed line) and from the TL + ionosphere system (solid line). The chosen parameters of TL correspond to TF-2 model, $\Sigma_{\rm IP} = 5.0$ Ohm$^{-1}$, $V_{\rm A} = 10^3$ km/s, $h1 = 1600$ km, $N = 10^9$ m$^{-3}$, $\omega = 2\pi/100$ s$^{-1}$. Under these parameters $\lambda_{\rm A} \simeq 0.5$ km.

For a given set of parameters the scale-dependences of the reflection coefficient and magnetospheric resonator

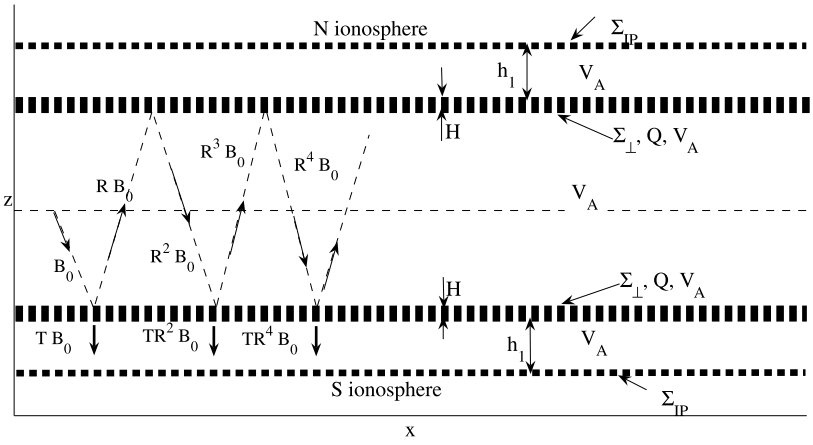


Fig. 7. Schematic illustration of the Alfven wave interaction with a TL + ionosphere system.

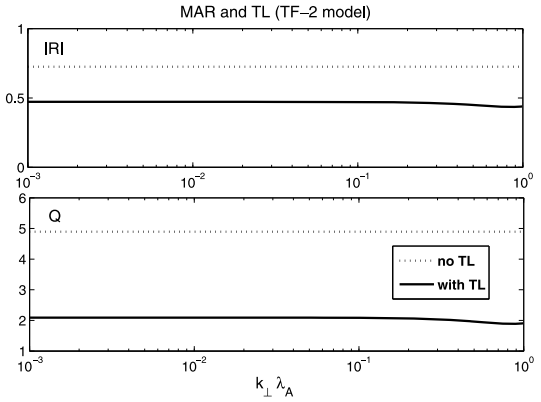


Fig. 8. Results of numerical modeling of the MAR with a TL: (a) coefficient of reflection from the ionosphere (dashed line) and from a TL + ionosphere system (solid line); (b) $Q$-factor of the MAR without a TL (dashed line) and with a TL (solid line).

quality $Q$ are shown in Fig. 8. The reflection coefficient of Alfven field line oscillations between conjugate ionospheres drops from ∼0.7 to ∼0.5 (Fig. 8(a)). The plot in Fig. 8(b) shows that the $Q$-factor of the MAR even with a thin TL (solid line) is more than 2 times less than without it (dotted line): ∼5 and ∼2. Upon growth of $k_\perp$ the $Q$-factor decreases until a minimal value is reached at $k_\perp \sim \lambda_A^{-1}$, and then increases under further growth of $k_\perp$ thanks to high reflection of small scale waves (this interval is of no interest for further consideration and is not shown in the figure).

Transverse scales of typical Pi2 pulsations as observed on the ground are much larger than $\lambda_A$. Therefore, damping of these oscillations is determined by the large-scale limit of dissipation on transverse resistance (49). Small-scale disturbances which may accompany Pi2 bursts are expected to be absorbed by the TL.

Thus, the occurrence of a TL with anomalous conductivity indeed results in a substantial increase of the Pi2 damping rate. However, the damping mechanism is different from the mechanisms proposed in earlier studies, and caused not by a field-aligned, but by transverse, anomalous resistance.

**4.3.1 Decay of quasi-static field-aligned currents** Turbulence can result not only in additional absorption of Alfven waves, but it can cause the divergence of quasi-static field-aligned currents. This effect destroys the electromagnetic coupling between the magnetosphere and ionosphere at small scales. From (16) it is possible to estimate the characteristic scale of current decrease due to divergence caused by static conductivity in a turbulent medium

$$\Delta z \simeq a_\perp \sqrt{\sigma_0/\sigma_P} \tag{58}$$

This relationship indicates that small-scale currents with a transverse scale $a_\perp$ will be totally screened by a TL with thickness $h > \Delta z$. For example, for TF-2 model parameters ($\sigma_0 = 2.9 \times 10^{-1}$ and $\sigma_P = 1.9 \times 10^{-6}$), a TL with thickness $\sim 10^3$ km causes substantial attenuation of field-aligned current structure with transverse scale <2.5 km.

## 5. Discussion and Conclusion

Satellite observations have confirmed that densities of currents transported by Alfven waves in the magnetosphere are sufficient for excitation of anomalous resistance and auroral form activation (Pilipenko *et al.*, 1999; Rankin *et al.*, 1999; Keiling *et al.*, 2002; Streltsov and Lotko, 2003).

Earlier theoretical estimates of plane Alfven wave damping (e.g., Liperovsky and Martjanov, 1973) were made under the assumption that anomalous resistance is evenly distributed along a flux tube. However, satellite observations show that turbulence is concentrated in a narrow layer above the auroral ionosphere (Fejer and Kelley, 1980). Alfven waves impinging on a TL with anomalous resistivity can partially reflect from it, be absorbed, and be transmitted through it. Considerations made in this paper extend the results of earlier works by Lysak and Dum (1983), and Trakhtenhertz and Feldstein (1985). When field-aligned resistivity dominates the relative effectiveness of these processes strongly depends on the wave transverse scale. A TL totally screens small-scale disturbances, and only weakly absorbs large-scale disturbances.

The basic features of the Alfven wave interaction with a TL are similar to those of the wave interaction with a multi-layer system including the auroral acceleration region (Vogt and Haerendel, 1998; Vogt, 2002). When the TL width is small as compared with the Alfven wave length, the key parameter which determines the effectiveness of the

wave interaction with a layer is the Alfven resistive scale $\lambda_A$. It is necessary to mention that the mechanisms of the influence on Alfven waves from the non-resistive potential drop (Vogt and Haerendel, 1998; Fedorov *et al.*, 2001) and from the anomalous resistivity, considered in this paper, are physically different. However, from the mathematical point of view, the reflection from the combined ionosphere-AAR system is formally very similar to those from the ionosphere-TL system with field-aligned resistivity. Surely, transverse conductivity does not occur in the AAR models, but it is of primary importance for the TL model considered here.

The analytical results obtained here may be applied to the description of the Alfven wave interaction either with a thin TL, when the field-aligned wave scale $L_\parallel$ is much larger than the TL width, $L_\parallel \gg h$ (Section 2.4), or in the local approximation, when $L_\parallel \ll h$ (Section 2.1). In the intermediate case, when $L_\parallel \sim h$, the model developed cannot be directly applied and a field-aligned dependence of the wave field and TL parameters is to be considered, which could be done only numerically.

Comparison of energy losses estimated from simplified analytical relationships for a thin layer, and numerically calculated from complete formulas for a finite width layer, has shown that the thin layer approximation gives reasonable estimates for all transverse wave scales, except very small. Estimation of the effective damping scale in a turbulent cusp shows that the cusp proper cannot be a conduit of Pc1-2 wave energy from the magnetosheath to the ground. This model also shows that the occurrence of anomalous transverse resistance when magnetospheric current exceeds the threshold necessary for the excitation of high-frequency plasma turbulence provides an additional non-linear damping rate of transient Pi2 pulsations.

At the auroral latitudes the convective plasma flow in the presence of a feedback between the magnetospheric disturbances and distortions of the ionospheric conductance can result in the instability of such system (Pokhotelov *et al.*, 2001; Lysak and Yoshikawa, 2006). In such situation a TL plays an important role providing an electron acceleration by anomalous $E_\parallel$. The necessary coupling between the magnetosphere and ionosphere for the feedback instability is performed by small-scale Alfven waves. However, the occurrence of TL providing an additional wave absorption and damping at small transverse sales (namely, at $L_\perp \leq \lambda_A$) can decouple the magnetospheric disturbances from the ionosphere. This effect, though it can influence significantly the development of feedback instability, has not been taken into account yet in the auroral physics.

**Acknowledgments.** This research is supported by NSF grant ATM-0305483 to Augsburg College (VAP, MJE) and INTAS grant 05-1000008-7978 (ENF). Stimulating discussions with V. Vovchenko and S. Shalimov, and comments of A. Yoshikawa and another reviewer are appreciated.

## References

Barsukov, V. M. and M. I. Pudovkin, Field-aligned conductivity and pulsation parameters, *Geomagn. Aeronomy*, **10**, 569–570, 1970.

Dyrud, L. P., M. J. Engebretson, J. L. Posch, W. J. Hughes, H. Fukunishi, R. L. Arnoldy, P. T. Newell, and R. B. Horne, Ground observations and possible source regions of two types of Pc1-2 micropulsations at very high latitudes, *J. Geophys. Res.*, **102**, 27011–27028, 1997.

Engebretson, M. J., T. G. Onsager, D. E. Rowland, R. E. Denton, J. L. Posch, C. T. Russell, P. J. Chi, R. L. Arnoldy, B. J. Anderson, and H. Fukunishi, On the source of Pc1-2 waves in the plasma mantle, *J. Geophys. Res.*, **110**, A06201, doi:10.1029/2004JA010515, 2005.

Erlandson, R. E., L. J. Zanetti, and T. A. Potemra, Observations of electromagnetic ion cyclotron waves and hot plasma in the polar cusp, *Geophys. Res. Lett.*, **15**, 421–424, 1988.

Fedorov, E., V. Pilipenko, and M. J. Engebretson, ULF wave damping in the auroral acceleration region, *J. Geophys. Res.*, **106**, 6203–6212, 2001.

Fedorov, E., V. Pilipenko, and V. V. Vovchenko, Interaction of Alfven waves with a resistive layer, *Geomagn. Aeronomy*, **47**, 606–615, 2007.

Fejer, B. G. and M. C. Kelley, Ionospheric irregularities, *Rev. Geophys. Space Phys.*, **18**, 401, 1980.

Fredricks, R. W., F. L. Scarf, and C. T. Russell, Field-aligned currents, plasma waves, and anomalous resistivity in the disturbed polar cusp, *J. Geophys. Res.*, **78**, 2133–2141, 1973.

Galeev, A. A. and R. Z. Sagdeev, Nonlinear plasma theory, in *Reviews of Plasma Physics*, edited by M. A. Leontovich, **N7**, 3–145, 1973.

Gudkova, V. A., L. M. Zeleny, and V. A. Liperovsky, About dynamics of field-aligned currents in the magnetosphere, *Geomagn. Aeronomy*, **13**, 318–324, 1973.

Gudkova, V. A., V. M. Barsukov, L. M. Zeleny, A. V. Volosevich, G. A. Loginov, and V. A. Liperovsky, Turbulence in the magnetospheric plasma and damping of Pi2 variations, *Geomagn. Aeronomy*, **14**, 764–766, 1974.

Hudson, M. K., R. L. Lysak, and F. S. Moser, Magnetic field-aligned potential drops due to electrostatic ion-cyclotron turbulence, *Geophys. Res. Lett.*, **5**, 143–146, 1978.

Ionson, J. A., Anomalous resistivity from electrostatic ion cyclotron turbulence, *Phys. Lett.*, **58A**, 105–107, 1976.

Keiling, A., J. R. Wygant, C. Cattell, W. Peria, G. Parks, M. Temerin, F. S. Mozer, C. T. Russell, and C. A. Kletzing, Correlation of Alfven wave Poynting flux in the plasma sheet at 4–7$R_E$ with ionospheric electron energy flux, *J. Geophys. Res.*, **107**, 1132, doi:10.1029/2001JA900140, 2002.

Kindel, J. M. and C. F. Kennel, Topside current instabilities, *J. Geophys. Res.*, **76**, 3055–3078, 1971.

Le, G., X. Blanco-Cano, C. T. Russell, X.-W. Zhou, F. Mozer, K. J. Trattner, S. A. Fuselier, and B. J. Anderson, Electromagnetic ion cyclotron waves in the high altitude cusp: Polar observations, *J. Geophys. Res.*, **106**, 19067–19080, 2001.

Liperovsky, V. A. and S. A. Martjanov, About damping of hydromagnetic waves in a turbulent plasma, *Geomagn. Aeronomy*, **13**, 311–317, 1973.

Liperovsky, V. A. and M. I. Pudovkin, Anomalous resistivity and double layers in magnetospheric plasma, Moscow, Nauka, p. 181, 1983 (in Russian).

Lotko, W., B. U. Ö. Sonnerup, and R. L. Lysak, Nonsteady boundary layer flow including ionospheric drag and parallel electric fields, *J. Geophys. Res.*, **92**, 8635, 1987.

Lyons, L. R., Generation of large-scale regions of auroral currents, electric potentials, and precipitation by the divergence of the convection electric field, *J. Geophys. Res.*, **85**, 17–24, 1980.

Lysak, L. R. and C. W. Carlson, Effect of microscopic turbulence on magnetosphere-ionosphere coupling, *Geophys. Res. Lett.*, **8**, 269–272, 1981.

Lysak, R. L. and C. T. Dum, Dynamics of magnetosphere-ionosphere coupling including turbulent transport, *J. Geophys. Res.*, **88**, 365–380, 1983.

Lysak, R. L. and A. Yoshikawa, Resonant cavities and waveguides in the ionosphere and atmosphere, in *Magnetospheric ULF Waves: Synthesis and New Directions*, *Geophys. Monogr. Ser.*, edited by K. Takahashi, P. J. Chi, R. E. Denton, and R. L. Lysak, **169**, 289–306, AGU, Washington, D.C., 2006.

Maltsev, Yu. P., Boundary conditions for Alfven waves on the ionosphere, *Geomagn. Aeronomy*, **17**, 1008–1011, 1977.

Mazur, N., E. Fedorov, V. Pilipenko, and A. Leonovich, Interaction of Alfven front with the plasma anomalous resistance layer, *J. Plasma Phys.*, **73**, 241–256, 2007.

Pilipenko, V., S. Shalimov, E. Fedorov, M. Engebretson, and W. Hughes, Coupling between field-aligned current impulses and Pi1 noise bursts, *J. Geophys. Res.*, **104**, 17419–17430, 1999.

Pokhotelov, O. A., V. Khruschev, M. Parrot, S. Senchenkov, and V. P. Pavlenko, Ionospheric Alfven resonator revisited: Feedback instability, *J. Geophys. Res.*, **106**, 25813–25824, 2001.

Rankin, R., J. C. Samson, and V. T. Tikhonchuk, Discrete auroral arcs and

nonlinear dispersive field line resonances, *Geophys. Res. Lett.*, **26**, 663–666, 1999.

Senatorov, V. A., Solution of the wave Alfven equation with account for finite conductivity and viscosity, *Geomagn. Aeronomy*, **36**, 164–165, 1996.

Shalimov, S. L. and V. A. Liperovsky, About saturation of turbulent energy density in field-aligned currents, *Space Res.*, **26**, 247–255, 1988.

Scholer, M., On the motion of artificial ion clouds in the magnetosphere, *Planet. Space Sci.*, **18**, 977, 1970.

Streltsov, A. V. and W. Lotko, Reflection and absorption of Alfvenic power in the low-altitude magnetosphere, *J. Geophys. Res.*, **108**, 8016, doi:10.1029/2002JA009425, 2003.

Swift, D. W., Mechanism for auroral precipitation: A review, *Rev. Geophys. Space Phys.*, **19**, 185–212, 1981.

Tikhonchuk, V. T. and V. Y. Bychenkov, Effect of anomalous resistivity on MHD wave damping, *J. Geophys. Res.*, **100**, 9535–9538, 1995.

Trakhtengertz, V. Yu. and A. Ya. Feldstein, About dissipation of Alfven waves in the layer with anomalous resistance, *Geomagn. Aeronomy*, **25**, 334–336, 1985.

Vogt, J., Alfven wave coupling in the auroral current circuit, *Surv. Geophys.*, **23**, 335–377, 2002.

Vogt, J. and G. Haerendel, Reflection and transmission of Alfven waves at the auroral acceleration region, *Geophys. Res. Lett.*, **25**, 277, 1998.

Yagova, N., V. Pilipenko, E. Fedorov, M. Vellante, and K. Yumoto, Influence of ionospheric conductivity on mid-latitude Pc3-4 pulsations, *Earth Planets Space*, **51**, 129–138, 1999.

V. Pilipenko (e-mail: pilipenk@augsburg.edu), E. Fedorov, and M. J. Engebretson